

Thermal, Mechanical, and Degradation Properties of Nanocomposites Prepared using Lignin-Cellulose Nanofibers and Poly(Lactic Acid)

Xuan Wang, Haibo Sun, Haolong Bai, and Li-ping Zhang*

A variety of nanocomposites were prepared using lignin-cellulose nanofibers (L-CNF) and poly(lactic acid) (PLA) via a solvent casting process. Acid hydrolysis and high-pressure homogenization processes were used to produce L-CNF from unbleached kraft pulps. Tensile tests were conducted on thin films, and the nanocomposites containing 3 wt. % L-CNF showed a 32.4% increase in tensile strength compared to that of neat PLA. Dynamic mechanical analysis showed that the tensile storage modulus increased in the viscoelastic temperature region with increasing L-CNF content in the nanocomposites. Thermogravimetric analysis (TGA) showed that all the materials investigated were thermally stable from 25 to 310 °C. Differential scanning calorimetry (DSC) showed a decrease in the cold crystallization temperature. A positive effect on the crystallization of PLA polymers in the nanocomposites with added L-CNF was observed using DSC and X-ray diffraction (XRD) analysis. The degradation profiles and swelling ratios of the nanocomposites improved.

Keywords: Poly(lactic acid); Lignin-cellulose nanofibers; Nanocomposites; Thermal properties

Contact information: College of Material Science and Technology, Beijing Forestry University, Beijing, 100083, PR China; *Corresponding author: zhanglp418@163.com

INTRODUCTION

Poly(lactic acid) (PLA) is a linear, aliphatic, thermoplastic polyester produced via ring-opening polymerization or polycondensation of lactic acid monomers. The monomers themselves can be obtained from fermentation of renewable resources such as corn, sugar beet, wheat, sugarcane, or any other starch-rich material (Anuar *et al.* 2012). Synthetic polylactic acid has been used for advanced applications in tissue engineering, food packaging, and drug delivery systems due to its great biodegradability, biocompatibility, and mechanical strength (Gupta *et al.* 2007). However, defects such as brittleness, low thermal stability, and low crystallization rate limit the applications of PLA. One way to improve the mechanical and thermal properties of the PLA is to add fiber and filler materials before it is used (Huda *et al.* 2006).

To prepare the PLA matrix, PLA is blended with reinforcing fibers. Polymers including starch (Martin and Avérous 2001), chatoyant (Mesquita *et al.* 2010), and inorganic fillers (Bleach *et al.* 2002) have also been added. Cellulose, a natural polymer obtained from plants, is both biodegradable and biocompatible. Cellulose nanowhiskers and nanofibers are the most common bio-based composite fillers. Cellulose nanofibers (CNF) have many positive qualities, such as good mechanical properties (*e.g.*, a Young's modulus of about 150 GPa) (Wu 2008) and high stiffness, aspect ratio, and relative surface area, that make it an attractive reinforcing material for biopolymers. However, the highly hydrophilic surface of cellulose makes it difficult to prevent fiber aggregation

within hydrophobic polymers such as PLA. To increase their compatibility, the surface of cellulose can be modified. Various surface modification techniques have been shown to improve the interaction at the interface between the PLA matrix and fibers, including esterification (Mohanty *et al.* 2001), acetylation (Khalil and Ismail 2000), and cyanoethylation (Sain *et al.* 2005).

It is well-known that the interfacial adhesion between polymers and natural fiber in composites can be improved using compatibilizers. Starch is one such example of a compatibilizer (Wang *et al.* 2002). Its effect on fiber-polymer compatibility is attributable to the introduction of reactive groups to the interface between the PLA matrix and the surface of the more polar starch particles. The chemical and physical interactions between the polar surfaces of starch particles and the less polar PLA host matrix were strengthened due to the formation of such an inter-phase. Oksman (2007) used polyvinyl alcohol to improve the dispersion of cellulose whiskers within the PLA matrix. The hydroxyl groups on partially hydrolyzed PVOH were expected to interact with the hydrophilic surfaces of the cellulose and the residual vinyl acetate groups within the PLA (Bondeson and Oksman 2007).

Lignin is a typical compatibilizer used in PLA-based composites. It is an amorphous macromolecule composed of repeating phenyl propane units with aliphatic and aromatic hydroxyl groups and carboxylic acid groups. Lignin is particularly interesting in this regard as it is a waste product of the paper industry (Wood *et al.* 2011). Previous work has shown that lignin can be used as an additive in composite fabrication *via* RTM (Resin Transfer Molding) technology. Wool *et al.* (2002) showed that lignin can impart beneficial properties to the structure of a composite when it is dissolved in aqueous sodium hydroxide (Thielemans *et al.* 2002). Graupner (2008) used lignin as an adhesion promoter in cotton fiber/PLA composites. Results indicated that lignin improves the fiber matrix adhesion in cotton fiber-reinforced PLA composites (Graupner 2008).

Lignin may improve CNF-to-PLA matrix adhesion and the structural properties of the resulting composite while minimizing the number of steps and chemical treatments required in production. This study investigated the effect of L-CNF on a PLA matrix, with a focus on the effects of L-CNF concentration and on improving mechanical properties. The thermo-mechanical properties, thermal stability, crystallization, and degradation properties of L-CNF/PLA nanocomposites were also investigated. Nanocomposites reinforced with 1, 3, and 5% L-CNF, prepared *via* a solvent casting process were examined.

EXPERIMENTAL

Materials

Unbleached Kraft wood pulp board (5% lignin content, produced *via* sulfate cooking) was purchased from a pulp and paper mill in Inner Mongolia, China. Poly(lactic acid) (PLA, M_w of 100,000, purchased from the Shanghai Yisheng Industry, Ltd.) was used as the matrix. N,N-dimethylacetamide (DMAc) and sulfuric acid (98%) were purchased from the Shantou Xilong Chemical Plant and the Beijing Chemical Plant, respectively.

Lignin Content Assessment

The half-scale kappa test method used in this experiment was based on the AS/NZS 1301.201.2002 method, the Papro 1.106 kappa number, and the TAPPI T236 standard (Beg *et al.* 2008)

L-CNF and Nanocomposite Preparation

Kraft pulp was pretreated in 15% sulfuric acid at a constant mixing speed of 150 rpm for 4 h at 85 °C, at a solid-to-liquid ratio of 1:20. The suspension was then vacuum-filtered, and the resulting cake was washed with deionized water to remove H⁺ and SO₄²⁻ ions, then with DMAc to remove water. After that, the cake was immersed in DMAc, and the pretreated lignin-containing cellulose suspended in the DMAc was homogenized at a pressure of 100 MPa for 10 cycles (Apparatus: GEA Niro Soavi, Italy). Through the combination of pretreatment and homogenization, the L-CNF was well-dispersed in the DMAc. The yield of the L-CNF from kraft pulp with acid hydrolysis and homogenized process was about 60%, and the lignin in the resulting L-CNF was tested with a result about 4% content.

The solvent-cast nanocomposites were prepared by dissolving PLA pellets in DMAc (16% w/v) and continuously stirring the mixture with a magnetic stirrer at 70 °C until the pellets were fully dissolved. Next, the L-CNF suspension was added to the DMAc and mixed thoroughly for 2 h. The formulations (see Table 1) were scraped with a scraper on glass and dried at 80 °C on an electric heating board. The composites obtained were placed under vacuum at 40 °C for 24 h to ensure that the solvent completely evaporated.

Table 1. Formulation and Sample Codes for the Nanocomposites Investigated in This Study

Sample Code	PLA (wt %)	L-CNF (wt %)
PLA	100	-
PLA-1	99	1
PLA-3	97	3
PLA-5	95	5

Characterization

Tensile testing

The nanocomposite films were prepared with dimensions of approximately 15×100 mm. The tensile properties were characterized using a DCP-KZ300 tensile test machine with a crossed head speed of 20 mm/min, gauge length 50 mm, and a 1 KN load cell. Five measurements were made for each specimen, and the data averaged to obtain a mean value.

Transmission electron microscope (TEM)

The L-CNF suspensions were deposited onto glow-discharged carbon-coated transmission electron microscopy grids and were negatively stained with 2% phosphotungstic acid. Images of the specimens were examined with a HITACHI H-600 transmission electron microscope at an acceleration voltage of 80 kV.

Dynamic mechanical analysis (DMA)

The thermomechanical properties of the PLA films and nanocomposites were measured using a dynamic mechanical analysis (DMA) instrument (Q800, TA Instruments, USA). The test specimens were prepared by cutting strips with width 10 mm and length 40 mm from the films. The tensile storage modulus and tan delta were measured at a frequency of 1 Hz, a strain rate 0.05%, and a heating rate of 5 °C over a temperature range of 0 to 100 °C. Three replicate samples were used to characterize each material.

Thermogravimetric analysis (TGA)

TGA was carried out using a thermogravimetric analyzer (TGA Q5000 IR) from room temperature (25 °C) to 500 °C, at a heating rate of 10 °C/min, under a 100 mL/min nitrogen gas flow. The weight loss (%) as a function of the temperature of freeze-dried L-CNF and nanocomposite films (6 to 10 mg) was determined.

Differential scanning calorimetry (DSC) analysis

The percentage of crystalline PLA in the nanocomposite films was determined using a DSC (Q2000, TA instruments, USA). A sample (of about 6 to 8 mg) was heated from 20 to 200 °C at a heating rate of 10 °C/min (for the first heating scan) and kept at 200 °C for 5 min. Next, the samples were cooled to 20 °C at 5 °C/min and were kept at 20 °C for 5 min before being heating once again to 200 °C at the same heating rate as before. A blank pan measurement was conducted to provide a baseline, and at least three tests were done for each material to ensure statistical validity. All data were acquired from the second heating cycle of the DSC scan to eliminate any potential effects of thermal history. The percentage crystallinity (X_c) of PLA in the nanocomposites was calculated according to Eq. 1,

$$X_c [\%] = [(\Delta H_m / \Phi_{PLA}) / \Delta H_m^0] \times 100 \quad (1)$$

where ΔH_m is the enthalpy of fusion (J/g) of the polymer nanocomposites, ΔH_m^0 is the enthalpy of fusion for a PLA crystal of infinite size (assumed to be 93.6 J/g), and Φ_{PLA} is the fraction of PLA in the nanocomposites.

X-ray diffraction analysis (XRD)

The XRD patterns of freeze-dried CNWs and nanocomposite films were obtained using an X-ray diffraction instrument (Shimadzu XRD-6000, Japan) operating at 30 kV and 15 mA with a Cu-K α radiation source ($k = 0.154$). The diffraction patterns were recorded for 2θ values between 5 and 40° using a step size of 0.04°, across 1200 steps, with a step time of 2 s. The degree of crystallinity of L-CNF was calculated according to Eq. 2,

$$I_c [\%] = [(I_{(Crys+am)} - I_{am}) / I_{am}] \times 100 \quad (2)$$

where $I_{(Crys+am)}$ is the peak intensity (counts per second) at roughly 22.8° for the crystalline and amorphous parts and I_{am} is the peak intensity at roughly 18°, representing the amorphous part of the CNF.

Degradation and swelling profile analysis

The degradation behavior of the nanocomposite films was evaluated by mass-loss measurement. The initial weight of three replicate samples of each material ($30 \times 5 \times 0.1$ mm) was measured before they were immersed in deionized water at different temperatures (25, 37, and 50 °C). After one week, samples were dried in a vacuum oven at 50 °C until a constant weight was reached. The percentage mass loss was determined according to Eq. 3,

$$\text{Mass loss [\%]} = [(M_o - M_{ds})/M_o] \times 100 \quad (3)$$

where M_o is the mass of the dry sample and M_{ds} is the mass of the dry sample after degradation.

The swelling ratios of the nanocomposites were determined by measuring the mass of the samples before and after swelling in deionized water for 1 week, according to Eq. 4,

$$\text{Swelling ratio [\%]} = [(M_w - M_o)/M_o] \times 100 \quad (4)$$

where M_w is the mass of the wet sample after swelling and M_o is the mass of the dry sample before swelling.

RESULTS AND DISCUSSION

Structure of Lignin-Cellulose Nanofibers

Figure 1 shows a transmission electron microscope image of L-CNF generated *via* sulfuric acid hydrolysis of unbleached kraft wood pulps. The length and width of L-CNF were determined from the TEM image and a large number of nanofibers were generated by acid hydrolysis. The average length of the L-CNF ranged from 400 to 600 nm, and the average nanofibers width derived from TEM measurements ranges from 20 to 50 nm, from which the aspect ratio of L-CNF, ranging from 12 to 20, can be obtained.

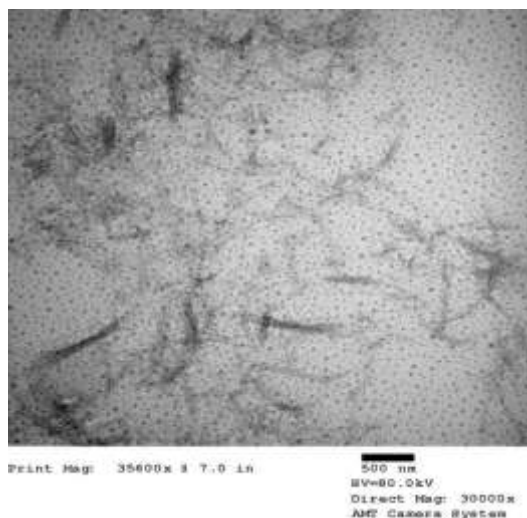


Fig. 1. The structure of the L-CNF analyzed with TEM

Mechanical Properties

The mechanical properties of the PLA composites reinforced with 1, 3, and 5 wt. % L-CNF and CNF (3 wt. %) were evaluated by tensile testing at room temperature. Figure 2 shows the effects of added CNF and L-CNF on the tensile strength and elongation at break of PLA composites. After addition CNF to PLA matrix, its tensile strength was decreased by 10.8% compared to that of neat PLA. This finding is attributable to poor interfacial bonding between the CNF and the PLA matrix (Masud *et al.* 2008; Qu *et al.* 2010). However, when the L-CNF was added to the PLA matrix, PLA-3 showed a significant increase (21.6%) in tensile strength, while PLA-1 and PLA-5 showed little increase compared to that of neat PLA. Neat PLA had a tensile strength of around 18.5 MPa. The elongation at break of all the composites investigated decreased as compared to that of the neat PLA. Reductions in elongation of 21.6%, 32.4%, and 54.1%, compared to the neat PLA, were seen for PLA-1, PLA-3, and PLA-5, respectively. It is possible that the nanoparticle filler made the PLA composites brittle (Shumigin *et al.* 2011).

It is known that the filler plays an important role in the mechanical properties of PLA/L-CNF composites. One of the main factors affecting the mechanical properties of L-CNF-reinforced material is the L-CNF-matrix interfacial adhesion. A weak interfacial region will reduce the efficiency of stress transfer from the matrix to the reinforcing component, lowering the composite's strength (Suarez *et al.* 2003).

The tensile strength testing results indicate that the addition of L-CNF reinforced the L-CNF/PLA composites. The tensile strength of composites first increased, then decreased with increasing L-CNF content, which can be seen in Fig. 2. It may be that lignin can improve the compatibility between PLA and CNF. The tensile strength change with changing L-CNF content could be due to better dispersion of the L-CNF within the composites. With high concentrations of L-CNF, poor dispersion occurred due to the strongly self-aggregating nature of L-CNF. This led to a less pronounced increase in tensile strength, a result very similar to those of Hossain *et al.* (2012).

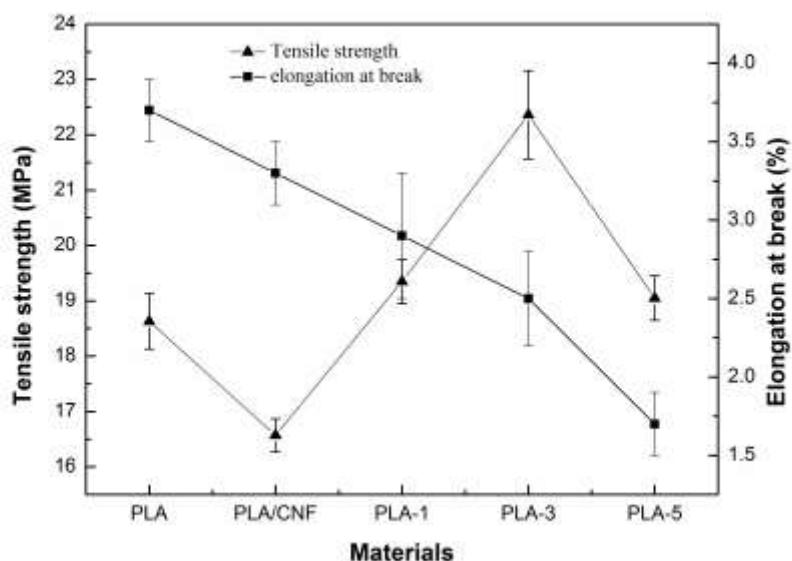


Fig. 2. Tensile strength and elongation properties of the PLA and nanocomposite films

Thermomechanical Properties

The thermomechanical properties of PLA nanocomposites were investigated *via* DMA to evaluate the mechanical behavior of nanocomposites with changes in temperature, especially in the plastic region of the polymer (Fig. 3).

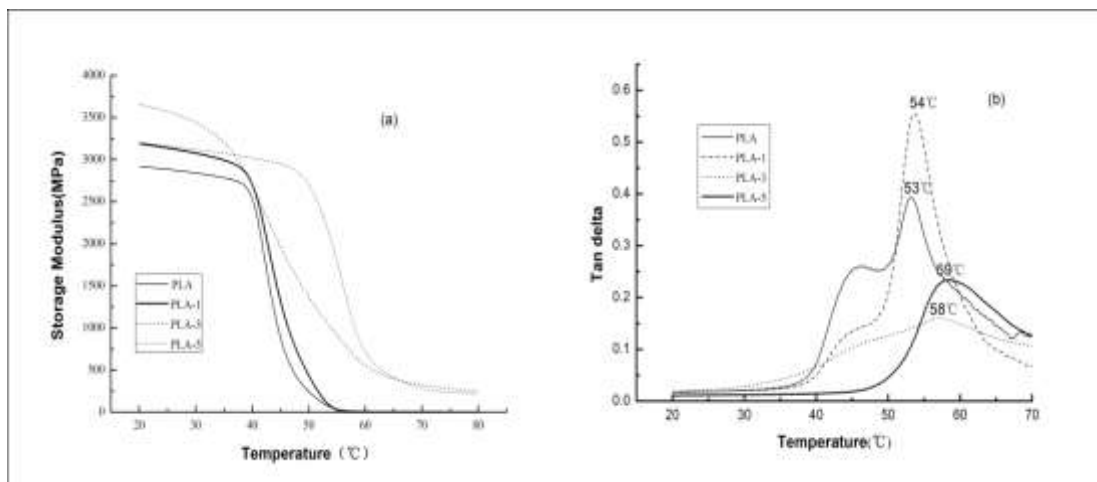


Fig. 3. (a) Tensile storage modulus curves from DMA data for neat PLA and composites, (b) tan delta curves from DMA data for neat PLA and composites

Figure 3a shows that the addition of L-CNF to the PLA nanocomposites increased the storage modulus as compared to the composites containing no additive. The incorporation of L-CNF in the PLA matrix improved the storage modulus for all nanocomposites in the viscoelastic temperature region of the polymer. Thus, the L-CNF content plays an important role in improving the storage modulus of the composites within the temperature regions investigated in this study. A 24% increase in storage modulus was observed at 25 °C in PLA-3 composites compared to neat PLA. This result is attributed to the superior interfacial adhesion between the matrix and L-CNF when the temperature remained below T_g . When PLA turned from a brittle, glassy material into a soft material as the temperature rose above T_g (Wang *et al.* 2012), its storage modulus quickly decreased. However, in the composites, structural integrity was maintained by the added L-CNF. The PLA-5 had the highest storage modulus when the temperature rose above T_g .

The tan delta peaks obtained for the nanocomposites investigated were seen to shift to the right, towards higher temperature regions, as compared to the tan delta peak for PLA alone (Fig. 3b). The tan delta peaks for PLA-1, PLA-3, and PLA-5 were seen at 54, 57, and 59 °C, respectively, compared to 53 °C for neat PLA, suggesting that the addition of L-CNF improved the storage modulus in the plastic region of the polymer. In accordance with the shifted tan delta peaks of the composites, the storage modulus of PLA-5 and PLA-3 remained high compared to those of PLA-1 and PLA alone when the temperature approached T_g . The rightward shift of the tan delta peaks also indicates that the reinforcement established in the composites had a significant effect on the segmental motion within the PLA matrix. This is attributed to a higher cross-linking density within the composites and surface-induced crystallization on the nanofibrils with an increase in L-CNF concentration. (Jonoobi *et al.* 2010)

Thermogravimetric Analysis (TGA)

Figure 4 shows the thermal stability of the L-CNF and PLA composites with different L-CNF contents. All materials were found to be thermally stable in the temperature region between 20 and 310 °C (Petersson *et al.* 2007). The L-CNF started to lose mass when the temperature exceeded 310 °C, similar to the temperature at which the composites began to decompose. Similar thermal behavior of CNF has also been reported in other literature (Qu *et al.* 2012; Roman and Winter 2004). The T_{onset} values for PLA, PLA-1, PLA-3, and PLA-5 were seen at 260, 251, 282, and 284 °C, whereas the T_{max} values for PLA, PLA-1, PLA-3, and PLA-5 were obtained at 356, 357, 359, and 352 °C.

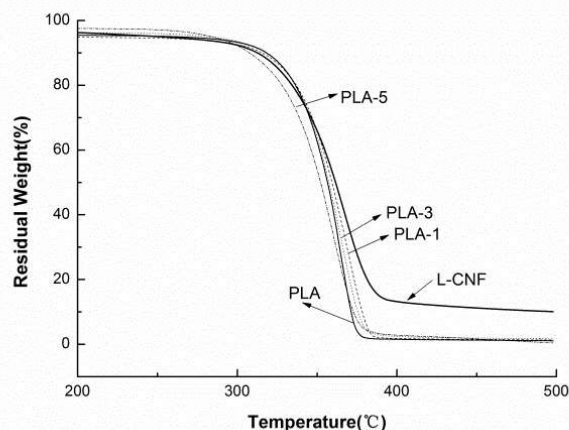


Fig. 4. TGA thermogram of the CNF, neat PLA, and composites investigated in this study

According to the data of T_{onset} and T_{max} for PLA composites, one can firmly conclude that PLA-3 had better thermal stability than PLA-1 and PLA-5, much like in the case of the mechanical properties of the PLA composites. PLA-3 exhibited good interfacial adhesion between CNF and PLA due to lignin, and the decreasing in thermal stability of PLA-5 was due to the self-reunited effect of L-CNF. At higher temperatures (around 400 °C), the residual weight-percent of the nanocomposites increased with increasing L-CNF content. The residual weight-percent values for PLA-1, PLA-3, and PLA-5 were 1.065%, 1.311%, and 1.677%, respectively, compared to 0.392% for neat PLA.

Differential Scanning Calorimetry (DSC)

DSC thermograms of PLA and PLA/L-CNF blends are shown in Fig. 5, and the thermal characteristics of each material are summarized in Table 2. Neat PLA displayed a glass transition temperature of 43.6 °C, while the addition of L-CNF resulted in a noticeable change in the glass transition temperature. This suggests that the PLA/L-CNF blends were very compatible (Byrne *et al.* 2009). A cold crystallization temperature was also observed for both neat PLA and PLA/L-CNF composite films. The T_{cc} value of the PLA/L-CNF blends shifted to lower temperatures with increasing L-CNF content. Neat PLA had a T_{cc} of 113.8 °C, but the addition of L-CNF noticeably decreased the T_{cc} . Increases and decreases in the T_{cc} of a component have been claimed to indicate more difficult or easier crystallization of that component, respectively, upon blending with another component (Taib *et al.* 2012). It could therefore be suggested that the addition of L-CNF increases the ability of PLA to crystallize or recrystallize.

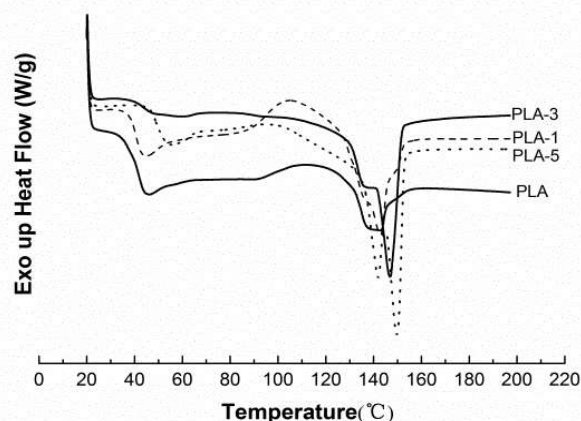


Fig. 5. DSC thermogram of the neat PLA and composites from the second heating run

Neat PLA had a shoulder peak at 138.5 °C and a melting peak at 142.6 °C. Various researchers have reported the existence of either two distinct melting peaks or a melting peak and a shoulder when performing DSC measurement of PLA or PLA blends with other polymers (Ren *et al.* 2006). During the DSC heating scan of neat PLA, the less-perfect crystals had enough time to melt and reorganize into crystals with greater structural perfection. The more stable crystals then remelted at higher temperatures (Jiang *et al.* 2006). The shoulder observed for PLA gradually changed to a peak with the addition of L-CNF. This suggests that a relatively larger number of less-perfect crystals in the nanocomposite films melted. The restriction of molecular segment mobility of the PLA decreased with increases in the L-CNF content.

Table 2 shows that ΔH_m and the degree of crystallinity (X_c) were improved by about 9 J/g and 10%, respectively, with the addition of L-CNF. The neat PLA was 16.9% crystalline. The percent crystallinity increased in the nanocomposites with 1%, 3%, and 5% added L-CNF by 19.4%, 26.5%, and 26.6%, respectively. Significant increases were not found as higher concentrations of L-CNF were used. Such an increase in crystallinity could be due to L-CNF promoting heterogeneous crystallization, effectively serving as a nucleating agent.

Table 2. Thermal Properties of Neat PLA and PLA Nanocomposites Generated by DSC (Second Heating at a Heating Rate of 10 °C/min)

Sample ^b	T_g (°C)	T_{cc} (°C)	T_m (°C)		ΔH_m (J/g)	X_c (%)
			1	2		
PLA	43.6	113.8	138.5	142.6	15.89	16.9
PLA-1	42.6	104.9	137.5	142.9	18.16	19.4
PLA-3	47.0	101.6	137.5	146.7	24.83	26.5
PLA-5	52.0	98.6	140.5	149.6	24.91	26.6

^a T_g , the glass transition temperature; T_{cc} , the cold crystallization temperature; T_m , the melting temperature; ΔH_m , the enthalpy of fusion; X_c , the degree of crystallinity.

^b PLA-to-L-CNF weight ratio.

X-ray Diffraction Analysis

Figure 6 shows the XRD patterns of the L-CNF and PLA nanocomposites. It reveals the crystallization properties of L-CNF and their effect on the crystallization of

PLA in the nanocomposites. As shown in the diffraction patterns of L-CNF, the highest peak was at a 2θ value of 22.6° and the double peak signal was at 2θ values of 14.9° and 16.5° . The peaks at 2θ values of 14.9° , 16.5° , and 22.6° were related to the (002) and (001) crystallographic planes, respectively. Both of the peaks could be attributed to cellulose I, which has a monoclinic structure. Lignin is an amorphous substance, and as such, the crystallinity index of L-CNF was only 59%.

The main diffraction peaks for neat PLA were seen at 2θ values of 16.5° and 18.9° , with a third, weaker peak at around 22.5° . These results are consistent with those of other studies (Yasuniwa *et al.* 2006). The XRD traces for the nanocomposites showed clear retention of cellulose crystallites with increasing peak intensities at 2θ values of 14.9° , 16.5° and 22.5° , which could be explained that the addition of L-CNF. This could be due to an increase in the crystallinity of the nanocomposites, consistent with the DSC results.

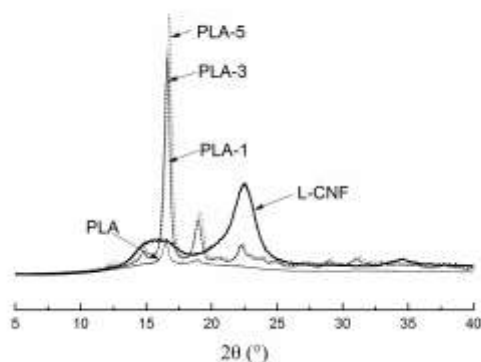


Fig. 6. XRD patterns of the L-CNF, neat PLA, and composites investigated in this study

Degradation and Swelling Properties

The degradation behavior of the nanocomposites after a week of immersion in deionized water at varying temperatures (25, 37, and 50 °C) is shown in Fig. 7. The percentage mass loss of PLA alone increased significantly with increasing temperature (up to approximately 5.2% at 50 °C). This loss was attributed to hydrolysis of the polymer, which was more thorough at higher temperatures. At room temperature, the mass loss of the nanocomposites increased with increasing L-CNF content as compared to that of PLA alone. However, at 37 °C in all nanocomposites, the percentage mass loss was slightly lower compared to the room temperature trials, perhaps due to hydrolysis and degradation of the amorphous domain of the polymer at higher temperatures. Further, nanocrystals may have reinforced the polymer interface and hindered the degradation of the nanocomposites. A significant percentage mass loss was observed at 50 °C for all nanocomposites tested, likely due to the leaching of L-CNF and the continuous breakdown of the interface between the L-CNF and the polymer matrix.

Figure 8 shows the swelling behavior of the nanocomposites immersed in deionized water at varying temperatures (25, 37, and 50 °C) for 1 week. The swelling ratio increased with increasing L-CNF content at all temperatures investigated. This effect was due to the increased hydrophilicity of the nanocomposites with the presence of L-CNF in the PLA matrix. The three-dimensional network between the nanofibers, formed by hydrogen bonding, was suggested to have a significant influence on the

swelling behavior of the nanocomposites, a conclusion also reported by de Rodriguez *et al.* (2006). A significant decrease in the swelling ratio of PLA alone at higher temperatures was observed due to the continuous degradation of PLA *via* hydrolysis. However, the presence of L-CNF in the nanocomposites increased the swelling ratio at 37 °C, which was due to an increase in the surface area within the nanocomposites caused by the addition of L-CNF and water accumulation at the PLA/L-CNF interface. At 50 °C, the swelling ratio decreased due to the degradation of PLA and the disruption of the PLA/L-CNF interface within the nanocomposites.

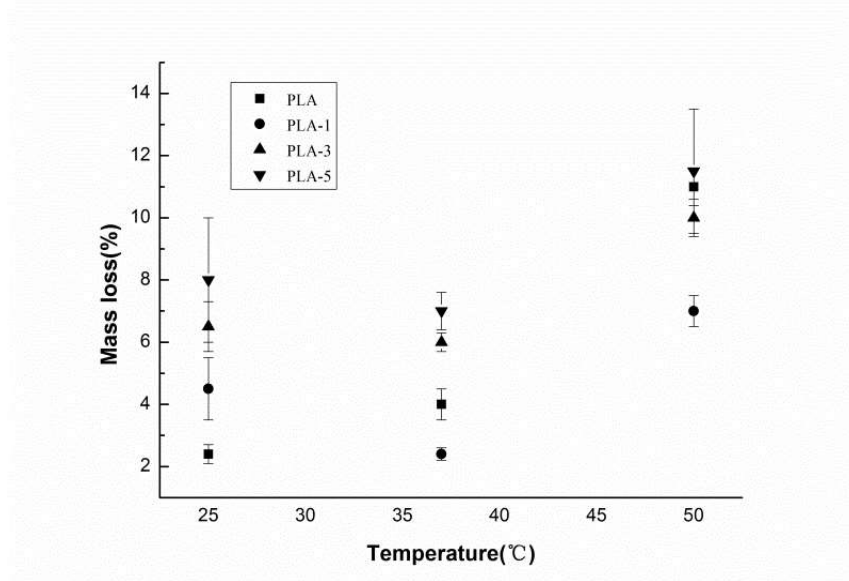


Fig. 7. Mass loss of nanocomposite films immersed in deionized water at different temperatures

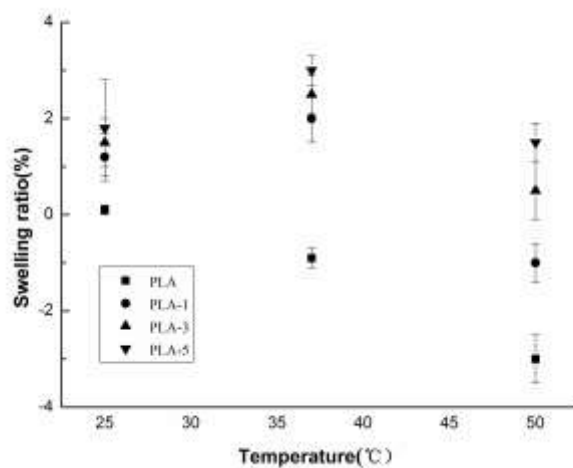


Fig. 8. Swelling ratio of nanocomposite films immersed in deionized water at different temperatures

CONCLUSION

1. This study demonstrated that nanocomposite films with good mechanical and thermomechanical properties can be successfully developed using L-CNF as a reinforcing agent with PLA as the matrix.

2. The mechanical properties, thermomechanical properties, and crystallinity of PLA/L-CNF nanocomposites were higher than those of the PLA matrix alone. With the addition of L-CNF, reinforcement and surface-induced crystallization were established in the nanocomposites. This was confirmed by tan delta curves in the plastic temperature region of the PLA.
3. The thermal stability of PLA/L-CNF nanocomposites improved compared to that of neat PLA. DSC results showed that the addition of L-CNF increased the ability of PLA to crystallize or recrystallize, resulting in an increased degree of crystallinity for the PLA and a shift the cold crystallization temperature to lower temperatures with increasing L-CNF content.
4. L-CNF in the nanocomposites had a significant influence on their degradation behavior at varying temperatures. The swelling ratio of the nanocomposites increased in all temperature regions investigated due to the addition of L-CNF.
5. The incorporation of L-CNF within a PLA matrix can improve the physical and chemical properties of PLA nanocomposites. Neat PLA and L-CNF are biocompatible, and the resulting nanocomposites could be useful for new PLA applications in the tissue engineering and food packaging fields.

ACKNOWLEDGMENTS

We are thankful for financial support for this research from the Doctoral Fund of the Ministry of Education of China (20110014110012) and the Beijing Natural Science Foundation (2112031).

REFERENCES CITED

- Anuar, H., Zuraida, A., Kovacs, J. J., and Tabi, T. (2012). "Improvement of mechanical properties of injection-molded polylactic acid-kenaf fiber biocomposite," *J. Thermoplastic Compos.* 25(2), 153-164.
- Beg, M. D. H., and Pickering, K. L. (2008). "Accelerated weathering of unbleached and bleached Kraft wood fibre reinforced polypropylene composites," *Polym. Degrad. Stabil.* 93(5), 1939-1946.
- Bleach, N. C., Nazhat, S. N., Tanner, K. E., Kellomaki, M., and Tormala, P. (2002). "Effect of filler content on mechanical and dynamic mechanical properties of particulate biphasic calcium phosphate-poly lactide composites," *Biomaterials* 23(7), 1579-1585.
- Bondeson, D., and Oksman, K. (2007). "Polylactic acid/cellulose whisker nanocomposites modified by polyvinyl alcohol," *Compos. Part A-Appl. Sci.* 38(12), 2486-2492.
- Byrne, F., Ward, P. G., Kennedy, J., Imaz, N., Hughes, D., and Dowling, D. P. (2009). "The effect of masterbatch addition on the mechanical, thermal, optical and surface properties of poly(lactic acid)," *J. Polym. Environ.* 17(1), 28-33.
- de Rodriguez, N. L. G., Thielemans, W., and Dufresne, A. (2006). "Sisal cellulose whiskers reinforced polyvinyl acetate nanocomposites," *Cellulose* 13(3), 261-270.
- Graupner, N. (2008). "Application of lignin as natural adhesion promoter in cotton fibre-

- reinforced poly(lactic acid) (PLA) composites,” *J. Mater. Sci.* 43(15), 5222-5229.
- Gupta, B., Revagade, N., and Hiborn, J. (2007). “Poly(lactic acid) fiber: An overview,” *Prog. Polym. Sci.* 32(4), 455-482.
- Hossain, K. M. Z., Ahmed, I., Parsons, A. J., Scotchford, C. A., and Walker, G. S. (2012). “Physico-chemical and mechanical properties of nanocomposites prepared using cellulose nanowhiskers and poly(lactic acid),” *J. Mater. Sci.* 47(6), 2675-2686.
- Huda, M. S., Drazl, L. T., Mohanty, A. K., and Misra, M. (2006). “Chopped glass and recycled newspaper as reinforcement fibers in injection molded poly(lactic acid) (PLA) composites: A comparative study,” *Compos. Sci. Technol.* 66(5), 1813-1824.
- Jiang, L., Wolcott, M. P., and Zhang, J. W. (2006). “Study of biodegradable polyactide/poly(butylene adipate-co-terephthalate) blends,” *Biomacromolecules* 7(1), 199-207.
- Jonoobi, M., Harun, J., Mathew, A., and Oksman, K. (2010). “Mechanical properties of cellulose nanofiber (CNF) reinforced polylactic acid (PLA) prepared by twin screw extrusion,” *Compos. Sci. Technol.* 70(12), 1742-1747.
- Khalil, S. A. H. P., and Ismail, H. (2000). “Effect of acetylation and coupling agent treatments upon biological degradation of plant fibre reinforced polyester composites,” *Polym. Test* 20(1), 66-75.
- Martin, O., and Avérous, L. (2001). “Poly(lactic acid): Plasticization and properties of biodegradable multiphase systems,” *Polymer* 42(14), 6209-6219.
- Masud, H. S., Lawrence, D. T., and Manjusri, M. (2008). “Effect of fiber surface-treatments on the properties of laminated biocomposites from poly(lactic acid) (PLA) and kenaf fibers,” *Compos. Sci. Technol.* 68(2), 424-432.
- Mesquita, J. P., Donnici, C. L., and Pereira, F. V. (2010). “Biobased nanocomposites from layer-by-layer assembly of cellulose nanowhiskers with chitosan,” *Biomacromolecules* 11(2), 473-480.
- Mohanty, A. K., Misra, M., and Drzal, L. T. (2001). “Surface modifications of natural fibres and performance of the resulting biocomposites: An overview,” *Compos. Interface* 8(5), 31-38.
- Petersson, L., Kvien, I., and Oksman, K. (2007). “Structure and thermal properties of poly(lactic acid)/cellulose whiskers nanocomposite materials,” *Compos. Sci. Technol.* 67(11), 2535-2544.
- Qu, P., Zhou, Y. T., Zhang, X. L., and Zhang, L. P. (2012). “Surface modification of cellulose nanofibrils for poly(lactic acid) composite application,” *J. Appl. Polym. Sci.* 125(4), 3084-3091.
- Qu, P., Gao, Y., and Zhang, L. P. (2010). “Nanocomposites of poly(lactic acid) reinforced with cellulose nanofibrils,” *BioResources* 5(3), 1811-1823.
- Ren, Z. J., Dong, L. S., and Yang, Y. M. (2006). “Dynamic mechanical and thermal properties of plasticized poly(lactic acid),” *J. Appl. Polym. Sci.* 101(3), 1583-1590.
- Roman, M., and Winter, W. T. (2004). “Effect of sulfate groups from sulfuric acid hydrolysis on the thermal degradation behavior of bacterial cellulose,” *Biomacromolecules* 5(5), 1671-1677.
- Sain, M., Suhara, P., Law, S., and Bouilloux, A. (2005). “Interface modification and mechanical properties of natural fiber-polyolefin composite products,” *J. Reinf. Plast. Comp.* 24(2), 121-130.
- Shumigin, D., Tarasova, E., Krumme, A., and Meier, P. (2011). “Rheological and mechanical properties of poly(lactic) acid/cellulose and LDPE/cellulose composites,” *Mater. Sci.* 17(1), 32-37.

- Suarez, J. C. M., Continho, F. M. B., and Sydenstricker, T. H. (2003). "SEM studies of tensile fracture surfaces of polypropylene - sawdust composites," *Polym. Test.* 22(7), 819-824.
- Taib, R. M., Ghaleb, Z. A., and Ishak, Z. A. M. (2012). "Thermal, mechanical, and morphological properties of polylactic acid toughened with an impact modifier," *J. Appl. Polym. Sci.* 123(5), 2715-2725.
- Thielemans, W., Can, E., Morye, S. S., and Wool, R. P. (2002). "Novel applications of lignin in composite materials," *J. Appl. Polym. Sci.* 83(2), 323-331.
- Wang, H., Sun, X. Z., and Seib, P. (2002). "Mechanical properties of poly(lactic acid) and wheat starch blends with methylenediphenyl diisocyanate," *J. Appl. Polym. Sci.* 84(6), 1257-1262.
- Wang, T., and Drzal, L. T. (2012). "Cellulose-nanofiber-reinforced poly(lactic acid) composites prepared by a water-based approach," *ACS Appl. Mater. Inter.* 4(10), 5079-5085.
- Wood, B. M., Coles, S. R., and Kerry, K. (2011). "Use of lignin as a compatibiliser in hemp/epoxy composites," *Compos. Sci. Technol.* 71(2), 1804-1810.
- Wu, C. S. (2008). "Characterizing biodegradation of PLA and PLA-g-AA/starch films using a phosphate-solubilizing *Bacillus* species" *Macromol. Biosci.* 8(6), 560-567.
- Yasuniwa, M., Tsubakihara, S., Iura, K., Ono, Y., Dan, Y., and Takahashi, K. (2006). "Crystallization behavior of poly(L-lactic acid)," *Polymer* 47(21), 7554-7563.

Article submitted: December 23, 2013; Peer review completed: March 6, 2014; Revised version received and accepted: March 19, 2014; Published: April 16, 2014.